

A Carbene–Carbene Complex Equilibrium

Robert A. Moss,* Lei Wang, Christina M. Odorisio, and Karsten Krogh-Jespersen*

Department of Chemistry and Chemical Biology, Rutgers, The State University of New Jersey, New Brunswick, New Jersey 08903

Received May 25, 2010; E-mail: moss@rutchem.rutgers.edu; krogh@rutchem.rutgers.edu

Abstract: Phenylchlorocarbene, generated by laser flash photolysis of phenylchlorodiazirine, formed highly stable π -type complexes with 1,3,5-trimethoxybenzene in pentane. The carbene and carbene complexes were in equilibrium. We measured the equilibrium constant ($K = 1264 \text{ M}^{-1}$ at 294 K) and, from its temperature dependence, extracted the associated thermodynamic parameters: $\Delta H^\circ = -7.1 \text{ kcal/mol}$, $\Delta S^\circ = -10.2 \text{ eu}$, and $\Delta G^\circ = -4.1 \text{ kcal/mol}$. The carbene complexes were characterized by UV–vis spectroscopy and computational analysis.

The search for transient carbene complexes has a venerable history. Indirect evidence in early reports highlights the modulation of carbenic reactivity and selectivity by electron-donating solvents such as dioxane, tetrahydrofuran (THF), benzene, or anisole.¹ Singlet carbenes deploy a formally vacant p orbital so that electron donation to this receptor by solvent heteroatoms or π -bonds provides a rationale for the observed solvent effects on reactivity, while computational studies support the formation of carbene–solvent complexes between, e.g., methylchlorocarbene and benzene or anisole.²

Direct observation of the complex provides stronger evidence for specific carbene solvation. Using photoacoustic spectroscopy, Kahn and Goodman detected heat deposition ascribed to the formation of a methylene–benzene π -complex.³ More recently, Platz et al. employed time-resolved IR spectroscopy to demonstrate formation of an *O*-ylide from an amidochlorocarbene and dioxane, suggesting the existence of a precursor carbene–dioxane complex.⁴

We used laser flash photolysis (LFP), coupled with UV–visible spectroscopy, to identify the spectroscopic signatures of transient carbene complexes formed between electron-rich aromatic ethers, such as anisole or 1,3,5-trimethoxybenzene, and halocarbenes, such as methylchlorocarbene,⁵ benzylchlorocarbene,⁵ *p*-nitrophenylchlorocarbene,⁶ and dichlorocarbene.^{7,8} Computational studies provided analyses of the absorption spectra and likely structures of the observed complexes.^{5–8} Here, we offer the first direct spectroscopic evidence for a carbene–carbene complex equilibrium, and we extract the associated thermodynamic parameters. Computational studies afford quantitative support for our analysis.

LFP of phenylchlorodiazirine⁹ in pentane affords phenylchlorocarbene (PhCCI), whose UV–vis spectrum features a strong $\pi \rightarrow \text{p}$ absorption at 308 nm and a weak $\sigma \rightarrow \text{p}$ absorption at 588 nm^{10,11} (cf. Figures S-2 and S-3 in the Supporting Information). LFP of the diazirine in the presence of 0.26 mM 1,3,5-trimethoxybenzene (TMB) gives the calibrated¹² UV–vis spectrum shown in blue in Figure 1, with a strong absorption at 324 nm and weaker absorptions at 484 and 596 nm ($\tau \approx 0.15 \text{ ms}$). Computational analysis (see below) of the PhCCI–TMB reaction enables us to assign the 484 nm absorption to specific PhCCI/TMB π -complexes A and B (see Figure 2). These carbene π -complexes also contribute

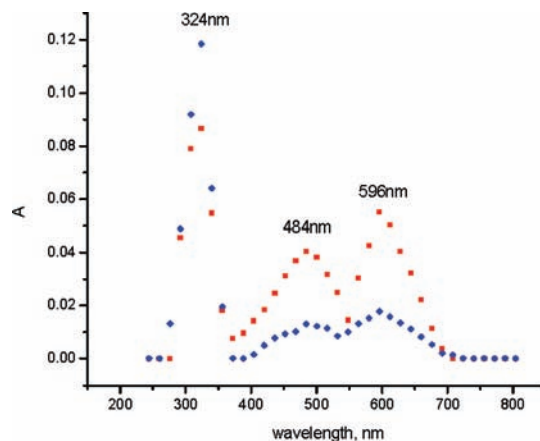


Figure 1. Calibrated¹² UV–vis spectra acquired 50 ns after LFP generation of PhCCI in TMB/pentane solution; blue spectrum at 0.26 mM TMB, red spectrum at 0.75 mM TMB.

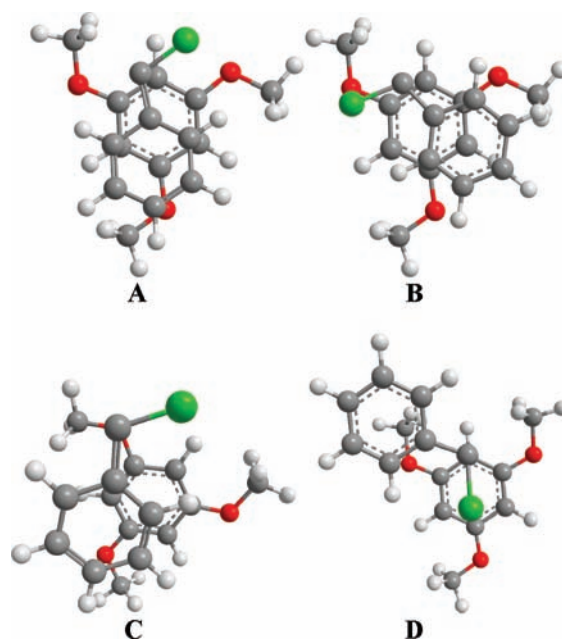


Figure 2. Four computed complexes formed between PhCCI and TMB (in perspective, carbene on top; green, chlorine; red, oxygen).

to the 324 nm absorption in Figure 1, although that signal is mainly due to PhCCI. The 596 nm absorption can be attributed mainly to these π -complexes, with a minor contribution from PhCCI.

The simultaneous appearance in Figure 1 of absorptions due to both PhCCI and PhCCI/TMB complexes suggests the establishment of a carbene–carbene complex equilibrium, eq 1. In accord with this idea, repetition of the PhCCI–TMB LFP experiment at 0.75

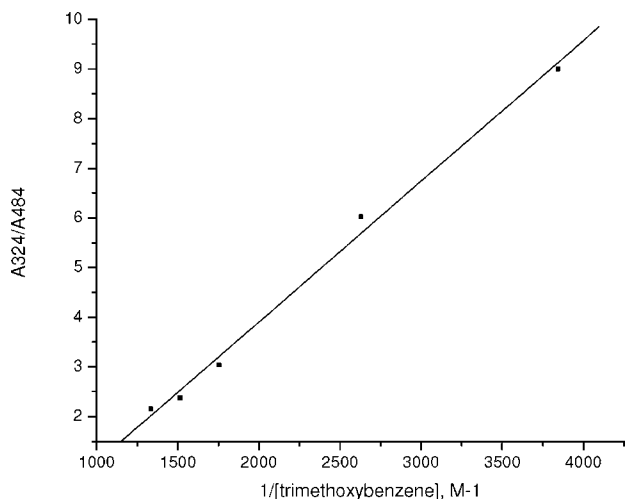


Figure 3. Relative absorption intensities at 324 nm/484 nm vs $1/[\text{TMB}]$ (M^{-1}) for the LFP generation of PhCCl in TMB/pentane solution at 294 K. The slope of the correlation line is $2.84 \times 10^{-3} \text{ M}$ ($r = 0.997$), leading to $K = 1264 \text{ M}^{-1}$ for eq 1.¹³

mM TMB affords the red spectrum in Figure 1. Comparison of the blue spectrum (0.26 mM TMB) with the red spectrum (0.75 mM TMB) reveals significant increases in the latter case of the 484 and 596 nm PhCCl–TMB π -complex absorptions versus the (mainly) PhCCl absorption at 324 nm.



Despite “contamination” of the 324 nm PhCCl absorption by the PhCCl–TMB complexes, it is possible to evaluate the contribution of the carbene alone by application of the Beer–Lambert law to the mixture of absorbers. The analysis, which ultimately employs the computed oscillator strengths (f) in place of the unknown extinction coefficients of PhCCl and PhCCl–TMB, is detailed in the Supporting Information. Accordingly, a plot of the quotient of the calibrated intensities of the 324 and 484 nm absorptions vs $1/[\text{TMB}]$ at 294 K gives the linear correlation of Figure 3, where the slope ($2.84 \times 10^{-3} \text{ M}$) leads to $K = 1264 \text{ M}^{-1}$ for eq 1.¹³

Formation of the PhCCl–TMB complexes from PhCCl and TMB is thus thermodynamically favorable ($K \gg 1$) at room temperature. We similarly determined K at four additional temperatures (see Figures S-7–S-10 in the Supporting Information), yielding the following values of K (M^{-1}): 4711 at 262 K, 2409 at 275 K, 1962 at 283 K, and 647 at 304 K. A plot of $\ln K$ vs $1/T$ appears in Figure 4, from which the slope and intercept give $\Delta H^\circ = -7.1 \pm 0.6 \text{ kcal/mol}$ and $\Delta S^\circ = -10.2 \pm 2.2 \text{ eu}$, respectively, leading to $\Delta G^\circ = -4.1 \pm 0.9 \text{ kcal/mol}$ (at 298 K). The thermodynamic parameters show that the equilibrium of eq 1 is enthalpy-driven in the direction of carbene complex formation.

Electronic structure calculations based on density functional theory provide structures and energetics of potential PhCCl–TMB complexes and rationalize their electronic absorption spectra. We have applied four density functional combinations (PBE,^{14a} B97D,^{14b} M06-2X,^{14c} and wB97XD^{14d}) and 6-311+G(d)¹⁵ basis sets in search of stable PhCCl–TMB complexes.¹⁶ Four minima (A–D, Figure 2; see Figure S-11 in the Supporting Information for additional views of complexes A–D) were located on the potential energy surface, and computed thermodynamic parameters obtained with the B97D functionals are shown in Table 1 (additional tables of thermodynamic data are available in the Supporting

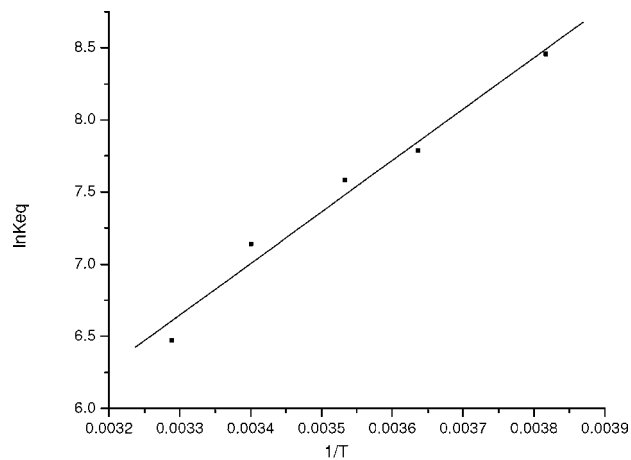


Figure 4. Plot of $\ln K$ (M^{-1}) vs $1/T$ (K^{-1}) for the equilibrium of eq 1. The slope (3570) affords $\Delta H^\circ = -7.1 \pm 0.6 \text{ kcal/mol}$, and the intercept (-5.13) gives $\Delta S^\circ = -10.2 \pm 2.2 \text{ eu}$. The correlation coefficient is $r = 0.988$.

Table 1. Thermodynamic Parameters for PhCCl–TMB Complexes Computed at the B97D/6-311+G(d) Level

species	ΔH° ^a	ΔS° ^a	ΔG° ^{a,b}	corr ΔH° ^{a,c}
A	−10.91	−35.8	−0.23	−8.16
B	−9.97	−34.7	0.37	−7.44
C	−8.59	−32.2	1.02	−6.43
D	−7.79	−34.2	2.42	−5.47

^a ΔH° and ΔG° in kcal/mol, ΔS° in eu, relative to the separated reactants; $T = 298.15 \text{ K}$. ^b The free energy differences were computed using a reference state of 1 M concentration for each species participating in the reaction. ^c Counterpoise corrected enthalpies.

Information as Tables S-1–S-4). The order of complex stability (**D** < **C** < **B** < **A**) was independent of which functionals were employed, but the enthalpies for carbene complex formation were much more favorable when one of the dispersion-corrected functionals was applied (B97D, M06-2X, or wB97XD). Moreover, the thermodynamic parameters produced by these latter functionals were very similar, despite the different approaches taken to include long-range, weak interactions (cf. Tables S-2–S-4). Three of the identified PhCCl–TMB complexes (**A**, **B**, and **D**) show the carbene carbon interacting with an unsubstituted carbon of TMB (C2); the fourth complex (**C**) features an ylidic-type C(PhCCl)–O(Me) interaction. The two most stable conformers (**A** and **B**) are both sandwich-type π -complexes involving substantial overlap between the aromatic ring moieties. Complexes **A** and **B** are nearly isoenergetic and structurally very similar; e.g., the computed C(PhCCl)–C2(DMB) distance is 2.77 Å in **A** and 2.96 Å in **B**. The more spatially extended complexes (**C** and **D**) are found at slightly higher energies (2–3 kcal/mol above **A**), and we consider these complexes to be noncompetitive at ambient temperature.

The binding enthalpies for complexes **A** and **B** computed at the B97D/6-311+G(d) level ($\Delta H^\circ \approx -10$ to -11 kcal/mol) are in fair agreement with the measured value ($\Delta H^\circ = -7.1 \text{ kcal/mol}$). Even better agreement with experiment is obtained when basis set superposition errors^{17a} are approximately accounted for via the counterpoise correction^{17b} (Table 1): $\Delta H^\circ = -8.2$ and -7.4 kcal/mol for **A** and **B**, respectively.

However, the computed entropies for complex formation are far more negative ($\sim -35 \text{ eu}$, Table 1) than observed (-10 eu). This may be largely ascribed to the different physical phases serving as references for the calculations (idealized gas phase) vs experiment (condensed phase). Due to the substantial overestimation of reaction entropies, the computed free energies of complexation ($\Delta G^\circ \approx 0$

Table 2. Electronic Transition Wavelengths (λ , nm) and Oscillator Strengths (f) (TD-B3LYP/6-311+G(d)//B97D/6-311+G(d) with CPCM^{18c} Solvent Correction (Heptane)) for PhCCl and PhCCl/TMB Complexes **A** and **B**

$\lambda(f)$	PhCCl	A	B
$\lambda_1(f_1)$	710(0.003)	666(0.023)	661(0.022)
$\lambda_2(f_2)$	336(0.037)	503(0.004)	507(0.001)
$\lambda_3(f_3)$	298(0.475)	430(0.154)	467(0.110)
$\lambda_4(f_4)$	278(0.000)	322(0.155)	336(0.040)
$\lambda_5(f_5)$	259(0.001)	317(0.063)	313(0.143)
$\lambda_6(f_6)$	237(0.010)	289(0.005)	291(0.127)

kcal/mol) become strongly dominated by the entropy term, and the computed equilibrium constant ($K \approx 1$) is consequently too small.

On the basis of the thermodynamic parameters presented in Table 1, we consider the significant absorption features in Figure 1 to arise exclusively from absorption by PhCCl and π -complexes of types **A** and **B** (Figure 2). The electronic transitions of lowest energy computed for these species are listed in Table 2 (TD-B3LYP/6-311+G(d)//B97D/6-311+G(d)).^{18a,b} PhCCl has a weak, broad $\sigma \rightarrow p$ absorption near 600 nm and a very intense $\pi(\text{Ph}) \rightarrow p$ charge-transfer absorption around 310 nm; TMB is spectroscopically silent above ca. 300 nm. Strong absorptions are computed for π -complexes **A** and **B** at 430 ($f = 0.15$) and 467 nm ($f = 0.11$), respectively, and we assign the absorption observed around 480 nm (Figure 1) to these species with confidence. Absorption from complexes **A** and **B** is mixed in with PhCCl absorption at longer wavelengths (>600 nm), as well as in the strong absorption peaking at 324 nm. The UV-vis excitations in complexes **A** and **B** originate in the π -system of DMB and terminate in the predominantly empty carbenic p orbital LUMO of PhCCl, and therefore they exhibit significant charge-transfer character. We note that the average of the f values for the **A** and **B** bands around 450 nm ($(0.154 + 0.110)/2 = 0.132$) and also the f value for PhCCl absorption computed at 298 nm ($f = 0.475$) are used in the numerical evaluation of the equilibrium constant for carbene complex formation (see the Supporting Information for details).

In conclusion, experimental and computational studies indicate that PhCCl, generated by LFP of phenylchlorodiazirine, forms highly stable complexes with TMB in pentane. We have measured the equilibrium constant, extracted the associated thermodynamic parameters for this carbene-carbene complex system, and characterized the complexes in detail by spectroscopic and computational analysis.

Acknowledgment. We are grateful to the National Science Foundation and to the Petroleum Research Fund for financial support.

Supporting Information Available: Figures S-1–S-11; Tables S-1–S-4; spectra calibration; equilibrium constant calculations; optimized geometries, absolute energies, electronic excitation energies, and oscillator strengths for all relevant computed species; and complete ref 16. This material is available free of charge via the Internet at <http://pubs.acs.org>.

References

- (1) (a) Tomioka, H.; Ozaki, Y.; Izawa, Y. *Tetrahedron* **1985**, *41*, 4987. (b) Ruck, R. T.; Jones, M., Jr. *Tetrahedron Lett.* **1998**, *39*, 2277. (c) Moss, R. A.; Yan, S.; Krogh-Jespersen, K. *J. Am. Chem. Soc.* **1998**, *120*, 1088.
- (2) Krogh-Jespersen, K.; Yan, S.; Moss, R. A. *J. Am. Chem. Soc.* **1999**, *121*, 6269.
- (3) Kahn, M. I.; Goodman, J. L. *J. Am. Chem. Soc.* **1995**, *117*, 6635.
- (4) Tippman, E. M.; Platz, M. S.; Svir, I. B.; Klymenko, O. V. *J. Am. Chem. Soc.* **2004**, *126*, 5750.
- (5) Moss, R. A.; Tian, J.; Sauers, R. R.; Krogh-Jespersen, K. *J. Am. Chem. Soc.* **2007**, *129*, 10019.
- (6) Moss, R. A.; Wang, L.; Weintraub, E.; Krogh-Jespersen, K. *J. Phys. Chem. A* **2008**, *112*, 4651.
- (7) Moss, R. A.; Wang, L.; Odorisio, C. M.; Krogh-Jespersen, K. *J. Phys. Chem. A* **2010**, *114*, 209.
- (8) Moss, R. A.; Wang, L.; Odorisio, C. M.; Krogh-Jespersen, K. *Tetrahedron Lett.* **2010**, *51*, 1467.
- (9) Graham, W. H. *J. Am. Chem. Soc.* **1965**, *87*, 4396. Phenylchlorodiazirine has maxima at 369, 384, and 389 nm; it was used with $A_{369} \approx 0.5$.
- (10) Turro, N. J.; Butcher, J. A., Jr.; Moss, R. A.; Guo, W.; Munjal, R. C.; Fedorynski, M. *J. Am. Chem. Soc.* **1980**, *102*, 7576.
- (11) Pliego, J. R., Jr.; De Almeida, W. B.; Celebi, S.; Zhu, Z.; Platz, M. S. *J. Phys. Chem. A* **1999**, *103*, 7481.
- (12) The intensities of the “raw” UV-vis absorptions are corrected for wavelength-dependent variations in sample absorptivity, xenon monitoring lamp emission, and detector sensitivity from 244 to 804 nm. For details, see Figure S-1 and the discussion in the Supporting Information.
- (13) $K = (1/\text{slope})(f_3/f_1)$, where f_3 (0.475) is the computed oscillator strength of PhCCl at 324 nm and f_1 (0.132) is the (average) computed oscillator strength of PhCCl-TMB π -complexes **A** and **B** at 484 nm. See the Supporting Information for details.
- (14) (a) Perdew, J. P.; Burke, K.; Ernzerhof, M. *Phys. Rev. Lett.* **1996**, *77*, 3865. (b) Grimme, S. *J. Comput. Chem.* **2006**, *27*, 1787. (c) Zhao, Y.; Truhlar, D. G. *J. Phys. Chem. A* **2006**, *110*, 5121. (d) Chai, J.-D.; Head-Gordon, M. *Phys. Chem. Chem. Phys.* **2008**, *10*, 6615.
- (15) (a) Ditchfield, R.; Hehre, W. J.; Pople, J. A. *J. Chem. Phys.* **1971**, *54*, 721. (b) Hariharan, P. C.; Pople, J. A. *Mol. Phys.* **1974**, *27*, 209. (c) Krishnan, R.; Binkley, J. S.; Seeger, R.; Pople, J. A. *J. Chem. Phys.* **1980**, *72*, 650. (d) McLean, A. D.; Chandler, G. S. *J. Chem. Phys.* **1980**, *72*, 5639. (e) Clark, T.; Chandrasekhar, J.; Spitznagel, G. W.; Schleyer, P. v. R. *J. Comput. Chem.* **1983**, *4*, 294.
- (16) All calculations made use of the Gaussian 09 program package: Frisch, M. J.; et al. *Gaussian 09*, Revision A02; Gaussian, Inc.: Wallingford, CT, 2009.
- (17) (a) Liu, B.; McLean, A. D. *J. Chem. Phys.* **1973**, *59*, 4557. (b) Boys, S. F.; Bernardi, F. *Mol. Phys.* **1970**, *19*, 553.
- (18) (a) Becke, A. D. *J. Chem. Phys.* **1993**, *98*, 5468. (b) Lee, C.; Yang, W.; Parr, R. G. *Phys. Rev. B* **1988**, *37*, 785. (c) Barone, V.; Cossi, M. *J. Phys. Chem. A* **1998**, *102*, 1995.

JA104514H